Demonstration of the Wilson–Bappu Effect

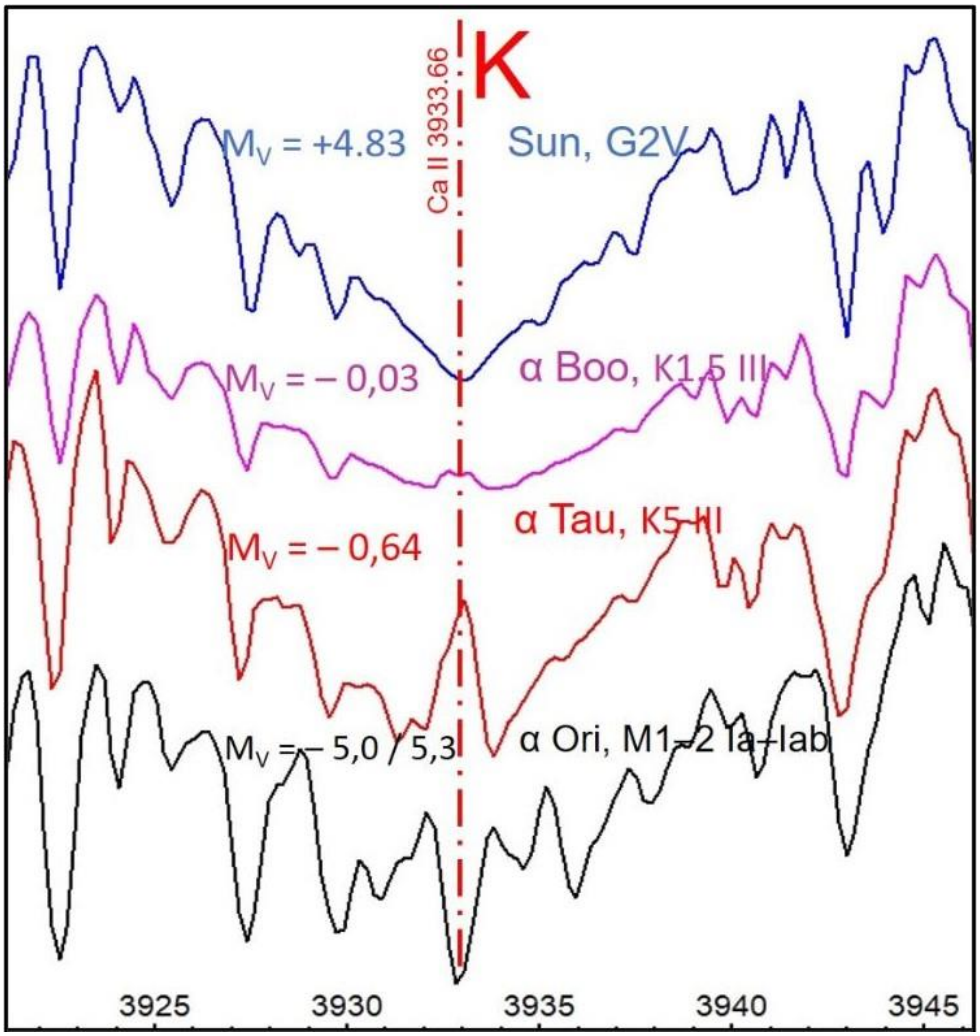

Version 1.0

Richard Walker 04/2022

Content

Cover photo: Central emissions in the core of Fraunhofer K absorptions.

1 Introduction

Focused on practical astro-spectroscopy, this topic has already been covered in the book Spectroscopy for Amateur Astronomers... [8] and will be supplemented and expanded here. The goal is a more detailed presentation of the method, as well as a purely qualitative demonstration of the Wilson-Bappu effect, without any scientific ambition.

2 Historical Aspects

In late F- to M-class stars, in high-resolution spectra narrow double-peaked emissions appare in the center of the impressive Fraunhofer H and K absorptions (Ca II λλ 3968.5 and 3933.6 Å). In 1957, the American O.C. Wilson and the Indian M. K. Vainu Bappu discovered a correlation between the half-width of these emissions and the absolute visual magnitude of the star. The derived empirical method then soon focused on the shorter wavelength K-line because at the longer wavelength H-absorption the emission often appears contaminated by other signatures. Moreover, the K line, within the stellar chromosphere, originates at a slightly higher level [5].

Fig. 1 shows from the original paper of 1957 [1] a small section of the evaluated spectra, which have been photographically recorded by the observatories Mt. Palomar and Mt. Wilson. The star designations have been supplemented here afterwards.

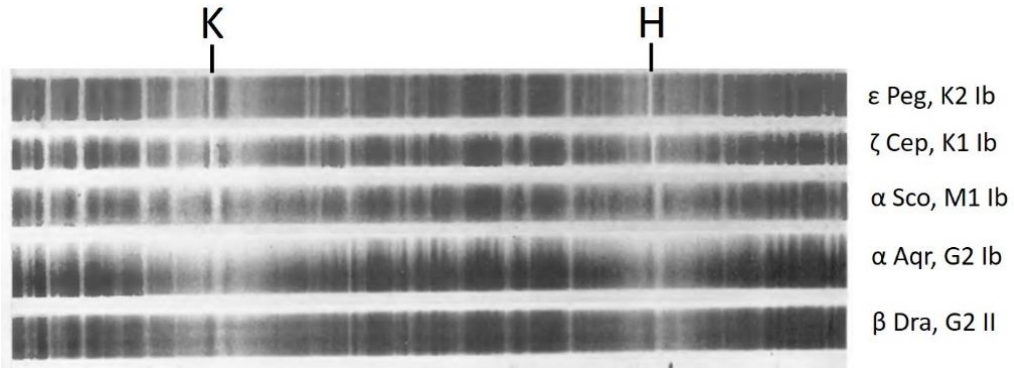

Abb. 1 Extract from the spectra analyzed by Wilson and Bappu [1]

The modest quality of these historical spectral images, reproduced here as negatives, impressively demonstrates the technological progress that has taken place until today, from which also amateurs may benefit. At that time, the stellar spectra, appearing to be line-shaped, had to be widened during the entire photographic exposure time by permanently moving the photographic plate. The measurement of the lines was done with special microscope-like equipment. Here recognizable as faint light gray zones, are the broad absorption sinks of the H- and K- lines, as well as the different width of the central emissions.

At that time, Wilson and Bappu studied 185 stars of spectral classes G to M. Purely empirically, this resulted in the linear relationship between the absolute, visual luminosities MV and the decadic logarithms of the measured half-widths log W_0, adjusted for instrumental broadening (Fig. 2). This connection is referred to in the literature as the *"Wilson-Bappu Relationship"* and is abbreviated as *"WBR"*.

Note: The WBR must not be confused with the Wilson effect, discovered already in the 18th century by Alexander Wilson, explaining the depression, visible within the spots observed near the solar limb.

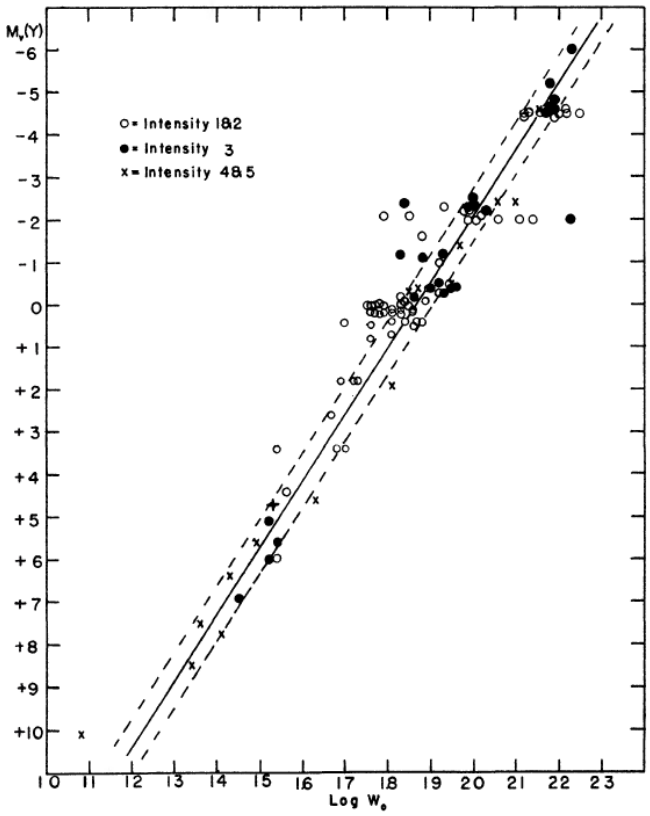

Fig. 2 WBR: Empirical linear relationship between the visual luminosities M_V and the decadic logarithms log W_0. Excerpt from the original paper from 1957 [1].

$$M_V \propto \log W_0$$

3 Origin and Significance of the Central Emission Peaks

The H- and K-absorptions of the ionized calcium Ca II are in the visual spectral range by far the most intense signatures within the spectral classes G - K. These broad absorption sinks, appearing superimposed with numerous slender metal lines, are generated mainly in the stellar photosphere.

However, the central, narrow double-peak emissions are generated in the higher-level chromosphere and therefore appropriately called "chromospheric" lines [5]. Their half-widths allow conclusions about the velocity of the stellar wind, outflowing within this layer. These emissions usually show an asymmetric double-peak profile with a self-absorption dip in between, generated by cooler gas layers, located on higher levels. (Figs. 3, 4).

In addition to the WBR, further analysis options exist, for example evaluating the asymmetry of the double peak.

4 Further Development of the WBR Method

Up to now, an impressive amount of research has been invested in this method [4], because WBR is also suitable for distance estimation based on the distance modulus [8]. The method has been continuously refined, as well as adapted to instrumental advances of the CCD spectra. For the following demonstration, the recalibration of the WBR by G. Pace et al [2] is applied:

$$M_V = 33{,}2 - 18{,}0\ log\ W_0 \qquad \{1\}$$

The measured half-width $FWHM_M$, of a line with wavelength λ, must first be corrected from the instrumental broadening $FWHM_{Instr}$. The corrected value $FWHM_{Korr}$ is obtained by formula {2} [8]:

$$FWHM_{Korr} = \sqrt{(FWHM_M)^2 - (FWHM_{Instr})^2} \qquad \{2\}$$

FWHM$_{Instr}$ is determined by the resolving power R of the spectrograph, i.e., the smallest possible width Δλ of a spectral signature at the wavelength λ that can still be resolved. If the R value of the spectrograph is known, *FWHM$_{Instr}$* can easily be calculated with formula {4} [8].

$$R = \frac{\lambda}{\Delta\lambda} \quad \{3\} \qquad FWHM_{Instr} = \frac{\lambda}{R} \quad \{4\}$$

Finally, the resulting *FWHM$_{Korr}$*, must be transformed into Doppler velocity [km/s] and is then denoted as W_0 [8]:

$$W_0 = \frac{FWHM_{Korr}}{\lambda} \cdot c \quad [km/s] \qquad \{5\}$$

5 Application Range for the WBR Method

The application of the WBR is limited to the late F- to M-class. Exclusively in this range, this spectral signature appears in such a way so it can be evaluated accordingly.

Further available for the WBR are the Mg II h- and k-lines in the UV range. However, these are inaccessible for amateurs and exclusively limited to space telescopes.

6 Demonstration of the WBR Method

6.1 Required Spectral Resolution

In order to make this signature visible, the spectral resolution must reach R>10'000. For the following experiments the directly coupled SQUES Echelle spectrograph was applied, here with a resolution of about 20'000. For this purpose, the variable slit width was set to about 50µm, striving for a compromise between resolution and exposure time. With presumably higher exposure effort, the Lhires III spectrograph equipped with the 2400 L/mm grating could also be suitable for this purpose. Professional investigations with the WBR are typically made with resolutions of R ≈ 60'000.

6.2 Possible Exposure Issues

Particularly with high-resolution spectrographs, challenges may arise with respect to exposure. Recording of the H- and K- lines are often hampered by the massive drop in sensitivity of current CCD cameras within the UV range. In addition, the later the spectral class, the more the focus of the stellar radiation flux gets shifted to the infrared domain.

6.3 Selection of the Analyzed Stars

For a pure qualitative representation of this effect, four stars with very different luminosity classes have been selected:

- Class V The main sequence star Sun
- Class III Arcturus and Aldebaran on the Giant Branch
- Class I The Supergiant Betelgeuse

Their apparent luminosity allows with a C8 telescope and in acceptable quality, the high-resolution recording of the H- and K-line. Spectroscopic multiple stars with relatively large secondary components have to be excluded, as they significantly affect the resulting luminosity. This includes e.g., the quadruple star Capella (α Aur) with the two main components of the classes G5 III + G0 III. The spectral classes and the apparent visual magnitudes m_v

are taken from the Simbad database [7], the absolute magnitudes M_v from the corresponding Wikipedia articles.

Star	m_v / M_v	Spectral class	Remarks
Sun	−26,74 / 4,83	G2V	Dwarf on the Main Sequence
α Boo / Arcturus	-0,05 / −0,3	K1.5 III	Red Giant
α Tau / Aldebaran	0,86 / −0,68	K5 III	Red Giant, long-term variable
α Ori / Betelgeuse	0,42 / −5,0 bis −5,3	M1-M2Ia-Iab	Red Supergiant, strongly variable

6.4 Profile Overview of the H- and K- Lines

For the selected "program stars" Fig. 3 shows an overview of the spectral profiles in the area of the H and K lines. The order is from top to bottom, according to the increasing absolute luminosity. It starts at the top with the Sun (M_v = +4.83) and ends at the bottom with the unstable Betelgeuse (M_v ≈ −5,0 to −5.3).

Independent of the spectral and luminosity class, the broadness and inclination of the absorption flanks, as well as the embedded metal lines, appear quite similar here. Relevant, however, is the clearly visible, and from the WBR postulated intensity increase of the central emission lines.

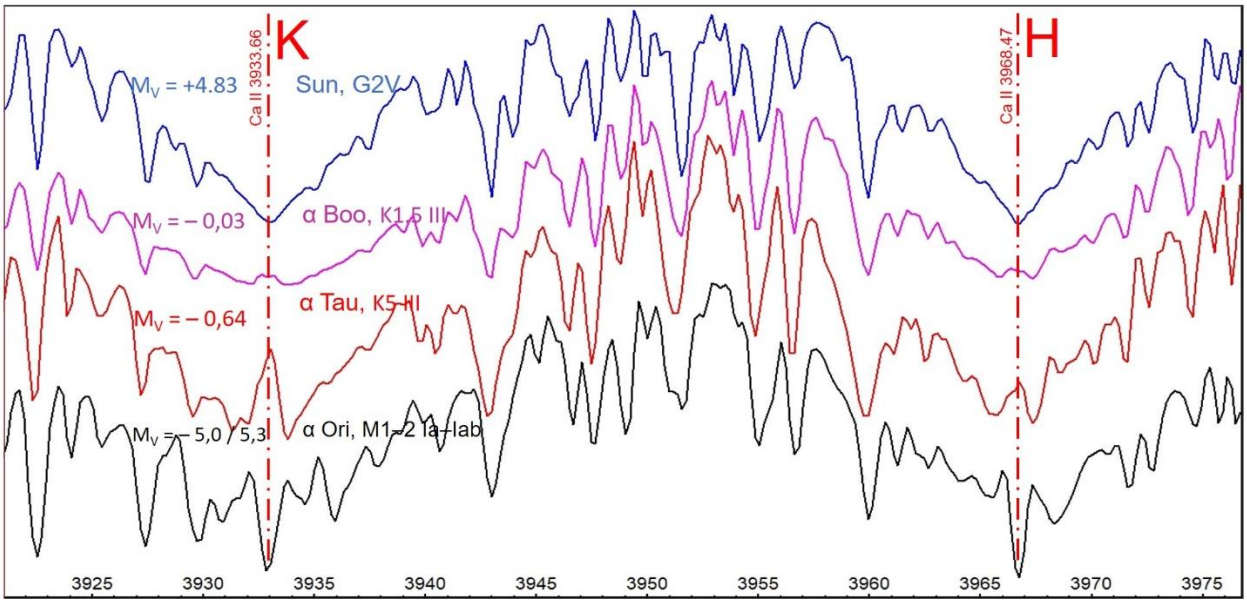

Fig. 3: Montage of the Ca II H- and K-lines for the Sun, Arcturus, Aldebaran, and Betelgeuse. For all profiles the course of the pseudocontinuum is rectified and the λ-shift corrected to the rest wavelength λ0.

6.5 Intensity and Shape of the Individual Emissions

The following can be seen in the highly zoomed line details of Fig. 4:

Sun: For the Sun, as a comparatively faint main sequence star, no emission can be detected because the spectral resolution of the spectrograph is here too low.

Arcturus (α Boo): In the K absorption of the Arcturus spectrum, there is a small, slightly asymmetric double-peak emission with a weak, central self-absorption dip between K2b and K2r. The short wavelength peak is here slightly more intense.

Aldebaran (α Tau): According to the higher luminosity M_v, the emission in the profile of Aldebaran is much more intense. It appears strongly asymmetric, i.e., the short wavelength peak is much weaker. Thus, the self-absorption dip between K2b and K2r appears strongly stretched.

Betelgeuse (α Ori): The Supergiant Betelgeuse exhibits intense self-absorption here, flanked by two faint emission peaks K2b and K2r.

6.6 Measuring the half-width *FWHM$_M$*

The measurement of *FWHM$_M$* is done here according to the pattern of G. Pace et al [2]. According to this, the measurement marks are located halfway between K1b and K2b for the blue flank and between K1r and K2r for the red flank. Details can be seen in Fig. 4.

To measure the wavelengths, a grid with a resolution of 0.1 Å was projected onto the profile. With a strong zoom on the central emissions to be evaluated, the profile course inevitably appears polygonal, corresponding to a dispersion of approx. 0.2Å/pixel (Fig. 4 left). The course of the polygon was therefore smoothed here approximately to a Bezier curve by the PowerPoint function "Smooth point" (Fig. 4 right).

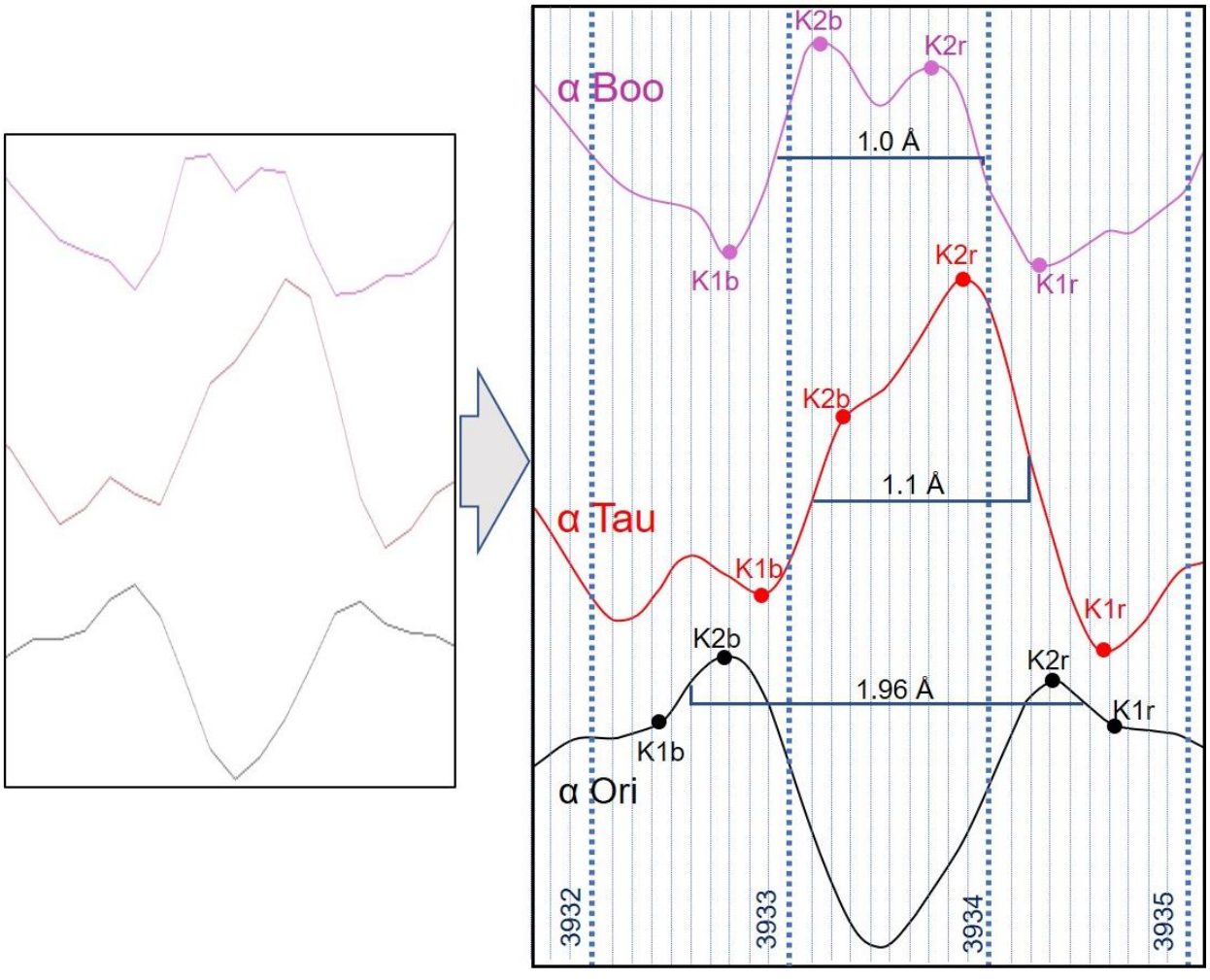

Fig. 4: Smoothing of the polygonal profile and 0.1 Å grid for measuring the half-widths

6.7 Mean Square Error of the WBR Method

According to [2] the mean square error of this method is indicated with 0.6 magnitudes.

7 Analysis

With the profiles of Fig. 3 and 4 the rough qualitative demonstration of the WBR is already completed. Here follows just a rough attempt to quantitatively evaluate the profiles by the formulas {1} to {5}. However, the relatively low-resolution and the small amount of data, does not allow a serious analysis. The calculated values for Mv here are all somewhat higher compared to those published. Further with increasing absolute luminosity, the deviation becomes larger.

Star	$FWHM_M$ [Å]	$FWHM_{Instr}$ [Å]	$FWHM_{Korr}$ [Å]	W_0 [km/s]	M_V WBR	M_V published	Difference [Mag]
Sun	$FWHM_M$ not measurable						
Arcturus	1,0	0,2	0,98	75	−0,5	−0,3	0,2
Aldebaran	1,1	0,2	1,08	82	−1,2	−0,68	0,52
Betelgeuse	1.96	0,2	1,95	149	−5,9	−5,0/ −5,3	0,9 0,6

8 Expansion of the WBR Method to Estimate the Surface Gravity.

In 2013, Sunkyung Park et al [3] showed that the Doppler velocity W_0 of the WBR method can also be used to determine the surface gravity log g of a star [8]. This additionally requires the effective temperature T_{eff} [8], which can be estimated from the spectral class [9]. It is calculated here as the decadic logarithm of the gravity g, expressed in cgs units [cm s^{-2}].

$$\log g = -5.85 \log W_0 + 9.97 \log T_{eff} - 23.48 \qquad \{6\}$$

9 Spectroscopic Determination of Luminosity for Early Spectral Classes

For the early spectral classes, the WBR method is not applicable. Valid from B0 - A5, the likewise empirical method according to Millward - Walker is available, which is based on the equivalent width EW of the Hγ-absorption [6], [8].

10 Literature

[1] O.C. Wilson, M.K. Vainu Bappu: *H and K Emission in Late-Type Stars: Dependence of Line Width on Luminosity and Related Topics, 1956*
https://articles.adsabs.harvard.edu/pdf/1957ApJ...125..661W

[2] G. Pace et al. *The Wilson–Bappu Effect: a Tool to Determine Stellar Distances.* 2002, Universita di Trieste, https://arxiv.org/pdf/astro-ph/0301637.pdf

[3] Sunkyung Park et al. *Wilson-Bappu Effect: Extended to Surface Gravity*, 2013
https://arxiv.org/abs/1307.0592

[4] Content of the NASA/ADS (Astrophysics Data System) to the Wilson Bappu Effect:
https://ui.adsabs.harvard.edu/search/p_=0&q=wilson%20Bappu%201957&sort=date%20desc%2C%20bibcode%20desc

[5] J.P. Biorgen et al. *Three-Dimensional Modeling of the Ca II H and K lines in the Solar Atmosphere*, A&A 2018, https://www.aanda.org/articles/aa/pdf/2018/03/aa31926-17.pdf

[6] G. A. Walker, Ch. G. Millward, *A Convincing Mv-W(Hγ) Calibration for A and B Supergiants*
https://articles.adsabs.harvard.edu/cgi-bin/nph-iarticle_query?1985ApJ...289..669W&defaultprint=YES&filetype=.pdf

[7] SIMBAD *Astronomical Database, CDS (Strasbourg)*
https://simbad.u-strasbg.fr/simbad/sim-fbasic

Author:

[8] M. F. M. Trypsteen, R. Walker: *Spectroscopy for Amateur Astronomers -Recording, Processing, Analysis and Interpretation*, 2017 Cambridge University Press, ISBN: 9781107166189

[9] R. Walker: *Spectral Atlas for Amateur Astronomers -A Guide to the Spectra of Astronomical Objects and Terrestrial Light Sources*, 2017 Cambridge University Press, ISBN: 9781107165908

Internet Documents by the Author

Various documents on the topic can be downloaded from the author's homepage:
https://www.ursusmajor.ch/astrospektroskopie/richard-walkers-page/index.html